IJCRT.ORG ISSN : 2320-2882

INTERNATIONAL JOURNAL OF CREATIVE RESEARCH THOUGHTS (IJCRT)

An International Open Access, Peer-reviewed, Refereed Journal

Optimization of Gas Tungsten Arc Welding Parameters to Improve Strength, Hardness and Corrosion Resistance of AA2219 Aluminium Alloy

[1]B Rajnaveen, [2]D Balaji Naik, [3]G Rambabu, [4]K Srinivasa Rao

[1, 3]Department of Mechanical Engineering, Andhra University, Visakhapatnam, [2]Department of Mechanical Engineering, Universal College of Eng. & Tech., Guntur, [4]Department of Metallurgical Engineering, Andhra University, Visakhapatnam, India

Abstract: For the fabrication of light weight structures, aluminium alloys are most suitable. And these alloys have high strength to weight ratio and have good corrosion properties. Gas tungsten arc welding (GTA) is a one of the most economical process of joining aluminium alloys which undergo physical, chemical and metallurgical transformations as a result of fusion welding. Taguchi method of experimental design was applied here to examine the effect of input parameters on strength, hardness and corrosion resistance. Input parameters like welding current, transitional speed and voltage are used as controlling parameters to create the experimental design and each parameter is divided into three levels. Therefore, an L_9 orthogonal array was used for the experimental design. Tensile, hardness and pitting corrosion tests were conducted as per the design matrix. Analysis of Variance (ANOVA) technique was used to determine the governing parameter of the process. The findings of ANOVA reveal that welding current is the most influencing parameter followed by voltage and transitional speed. Further, response surface methodology (RSM) has been used to form the mathematical model of AA2219 aluminium alloy. This mathematical model was helpful to find the predicted value of responses. The optimized parameter of AA2219 aluminium alloy was obtained by using RSM. The outcomes of RSM indicates that maximum strength, hardness and corrosion resistance is achieved when welding current, transitional speed and voltage are chosen as 150A, 70 mm/min, 31.68 kV respectively.

***Index Terms* - AA2219 alloy, gas tungsten arc welding, welding current, transitional speed, voltage, corrosion resistance, Taguchi design, Response surface methodology.**

I. INTRODUCTION

Aluminium alloys are the most often utilised materials in aircraft applications. A wide variety aluminium alloys are used to make riveted structural parts that meet certain needs, like high strength and high damage tolerance. However, the necessity to reduce aircraft weight and manufacturing costs has prompted the development of integrally stiffened metallic structures [1-6]. Another significant method of weight reduction has been accomplished through the development of superior precipitation-hardened aluminium alloys such as Al-Cu, Al-Mg-Si, and Al-Zn-Mg. AA2219 was developed in 1954 and has mostly succeeded AA2025 alloy. It comprises 6.03 % Cu, 0.23 % Mn, 0.11 % Zr, 0.09 % and 0.06 % Ti. In addition to its high strength-to-weight ratio and excellent cryogenic qualities, the AA2219 alloy offers a wide strength range (170 to 475 MPa). Liquid cryogenic rocket fuel tanks are most commonly constructed with AA2219 alloy [7]. However, in aluminium alloy welds. The resistance to corrosion is influenced by the alloy being welded, filler utilized and the welding technique used. It can be seen that the corrosion attacks are more localized. In some regions there is perforation of the samples, showing very poor corrosion resistance. Hence the pitting potential characteristic of aluminium alloys in the gas tungsten arc (GTA) welds becomes a serious issue [8-10]. The galvanic coupling induced by variations in electro chemical potentials between the matrix and precipitates and intermetallics of the base metal is commonly considered as the primary cause of joint corrosion [11]. As intermetallics with copper have different electrochemical characteristics than the matrix, they reduce the metal's localized corrosion resistance to seawater [12].

Many studies has been done on gas tungsten arc welded AA2219 alloy particularly on optimization of parameters as well as the evaluation of mechanical properties [13-14]. It has been discovered that copper distribution within the matrix is more uniform in gas tungsten arc welds resulting in better mechanical properties [15]. For TIG welding, Zhuang and Tong [16] used the modified Taguchi technique to evaluate the effectiveness of various welding factors like welding current, flow rate, arc gap and speed in determining the weld pool geometry. Due to phase transition induced by high temperatures encountered by the material, mechanical characteristics in the weld bead and HAZ have deteriorated in TIG welded AA2024 joints. The hardening sediments were primarily affected by TIG, leading to a major reduction in TIG welding's mechanical properties [17]. The joint's microstructure and mechanical properties depend on the heat produced by different welding parameters [18]. Despite superior mechanical properties, electron beam welded joints also suffer with fusion welding defects [19]. However, addition of copper to aluminium improves its overall strength, but it has a significant negative on the metal's corrosion resistance. The surface of metallic copper is highly efficient at reducing oxygen, and therefore, copper-rich sites allow oxygen and proton reduction reactions to occur with an enhanced efficiency, thus increasing the probability of stable pit growth [20]. Furthermore, the microstructure and different welding parameters have a significant impact on the corrosion behaviour.

Although very few information has been published regarding welding parameters' combined effects on the strength, hardness, and corrosion resistance of AA2219 al-alloy gas tungsten arc welds, the present work aims to optimize welding parameters to improve the qualities of AA2219 al-alloy gas tungsten arc welds.

II. EXPERIMENTAL DETAILS

2.1 Material and methods

The material used in the present investigation was high strength AA2219 Aluminium alloy in T87 temper condition of size 310mm X 150mm X 7mm and is procured from Vision Castings & Alloys Pvt Ltd in Hyderabad. The element composition of after testing AA2219 is shown in table 1. A gas tungsten arc welding machine was used to longitudinally butt weld the plates. Tensile, hardness and pitting corrosion tests are conducted after welding process.

Table 1 Element Composition (%Wt.) of Base Metal AA2219-T87 Al-alloy

Material	Cu	Mg	V	Fe	Si	Ti	Mn	Zr	Al
AA2219	6.08	0.01	0.09	0.10	0.07	0.06	0.23	0.11	93.2

3.2 Pitting Corrosion Test

Pitting corrosion resistance of AA2219 alloy welds was determined using Gill AC potentiostat and is shown in Fig. 1. 3.5% NaCl solution was used for all the pitting corrosion experiments with standard electrodes of calomel and pure graphite. Potential scan speed of 0.166 mVs^{-1}, pH of 10 and exposure area of 1 cm^2 were used and the potential at which sudden increase in current occurs is considered as critical pitting potential. Better pitting resistance is indicated by the higher positive potential value. Potentio dynamic polarization curves are obtained upon testing’s to correlate the pitting corrosion resistance.

Fig. 1 Basic Electrochemical System for corrosion testing (Gill AC)

III. TAGUCHI AND RSM

3.1 Taguchi Design

Systematic data is more likely to be obtained via a well-planned set of experiments, in which all relevant parameters are adjusted over a pre-determined range. However, the fact that process characteristics are being presented is typical and understandable due to the nature of the welding process as well as the noise of vibration.

Table. 2 Parameters and levels

S. no	Parameter	Notation	Unit	Levels		
				1	2	3
1	Welding current	WC	A	150	200	250
2	Transitional speed	WS	mm/min	50	60	70
3	Voltage	WV	V	20	30	40

The ranges of gas tungsten welding parameters were studied to construct a mathematical (regression) equation for corrosion resistance values. Table 2 lists the GTAW parameters and their respective levels.

Table 3 shows the Taguchi L_9 orthogonal array for three parameters each one at three levels. Using the design of experiments and RSM in Mini-tab software, a mathematical equation was created utilizing Table. 3 as input data.

Table 3 GTAW design matrix with experimental results

Experiment Number	Parameters			Ultimate tensile strength (Mpa)	Hardness (BHN)	Corrosion Pit Potential (mV)
	WC	WS	WV			
1	150	50	20	275	119	-570
2	150	60	30	250	115	-602
3	150	70	40	324	126	-542
4	200	50	30	185	98	-454
5	200	60	40	163	85	-561
6	200	70	20	212	103	-510
7	250	50	40	235	110	-415
8	250	60	20	155	80	-506
9	250	70	30	178	92	-472

3.1 RSM

RSM is indeed a set of statistical and mathematical approaches for modelling and analyzing the events in which the desired response is influenced by several variables, with the goal of optimizing that response. The responses (strength, hardness and Corrosion resistance) can be defined as a function of welding current (WC), transitional speed (WS) and voltage (WC)

Ultimate tensile strength (TS) = f (WC, WS. WV)

Hardness (BHN) = f (WC, WS, WV)

Corrosion resistance (CR) = f (WC, WS, WV)

The response CR is expressed by using regression equation

TS = 2091 - 6.277 WC - 36.33 WS - 10.12 WV + 0.0198WC*WC + 0.4 WS*WS + 0.095 WV*WV - 0.054 WC*WS + 0.022 WC*WV --- (1)

BHN=513.0 - 1.327 WC - 8.233 WS - 1.517 WV + 0.0046 WC*WC+ 0.1067 WS*WS - 0.031 WV*WV- 0.021WC*WS + 0.016 WC*WV --- (2)

CR=715.0 + 6.130 WC - 71.70 WS + 15.60 WV - 0.003800 WC*WC+ 0.6667 WS*WS - 0.2067 WV*WV - 0.05067 WC*WS - 0.01667 WC*WV --- (3)

Equation (1), (2) and (3) represents regression equation for tensile strength, hardness and corrosion resistance expressed as function of input factors. Main and interaction effects are considered for each parameter. The parameters are tested at 95% confidence level for their significance by using Minitab software package. It is possible to calculate the R^2 (coefficient of correlation) to see how well an experimental value fits a predetermined value [21]. The R^2 values, in this case, is 0.95, 0.90 and 0.93 for tensile strength, hardness and corrosion resistance respectively which indicating that the model only explains 1% of all variances.

3.3. Contour and response surface plots

In the evaluation of the response surface, contour plots are extremely useful. The experimenter can readily characterize the form of the surface and determine the optimum with reasonable precision by developing contour plots for response surface analysis using Minitab software. In most of the cases**,** the contour plots shows the less interaction between the factors but the interaction effects are observed in case of hardness contour plots (Fig. 3). These plots can be drawn with Minitab software by varying two parameters while other is held constant. The study of a response surface is analogous to "climbing a hill" to find the maximum response. The optimum point of minimum response was decided by the "descending into a valley". A saddle point, a maximum response point, or a maximum response point could all be represented by the stationary point [22]. The response surface plots for responses are obtained as shown in Fig. 5-7. These plots depict the optimum welding conditions at apex for gas tungsten arc welding process to achieve maximum of strength, hardness and corrosion resistance. It is also observed that there exists two way variation between the welding factors on responses.

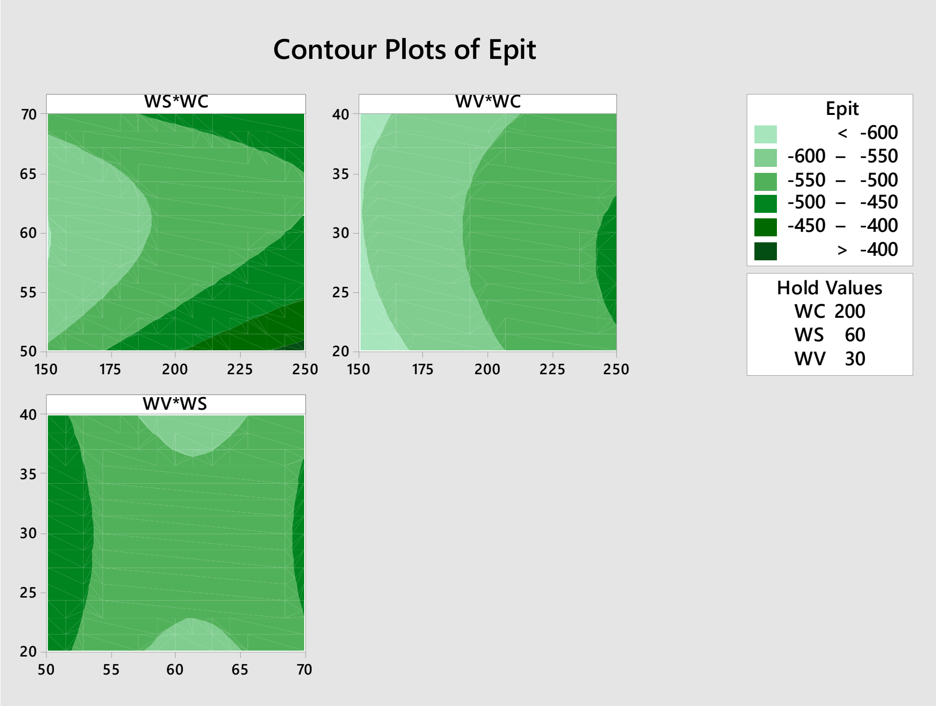

Fig. 2 Contour plot for CR

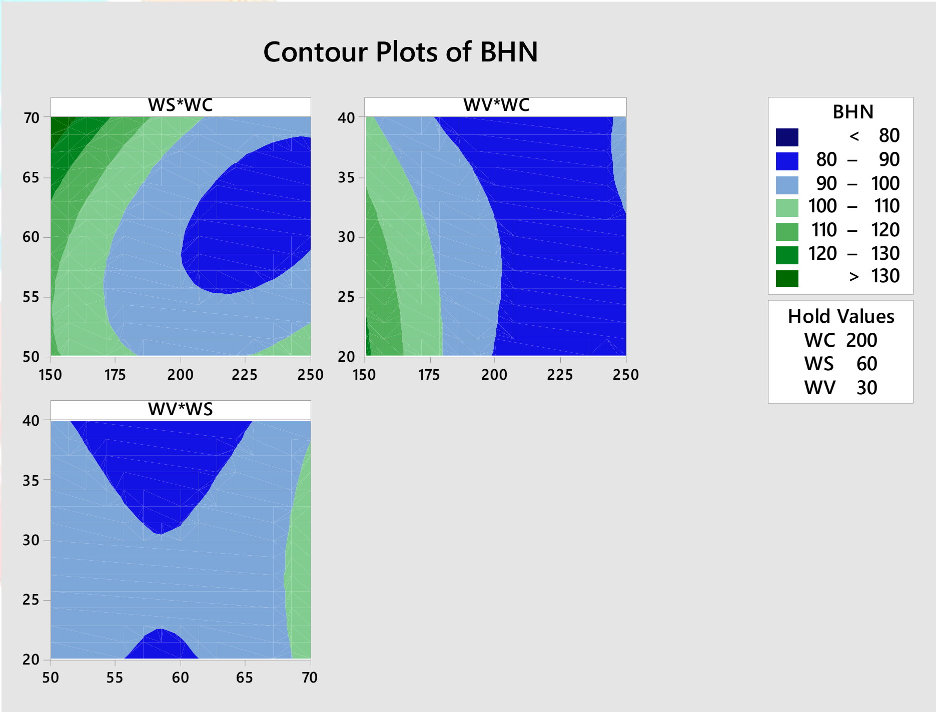

Fig. 3 Contour plot for BHN

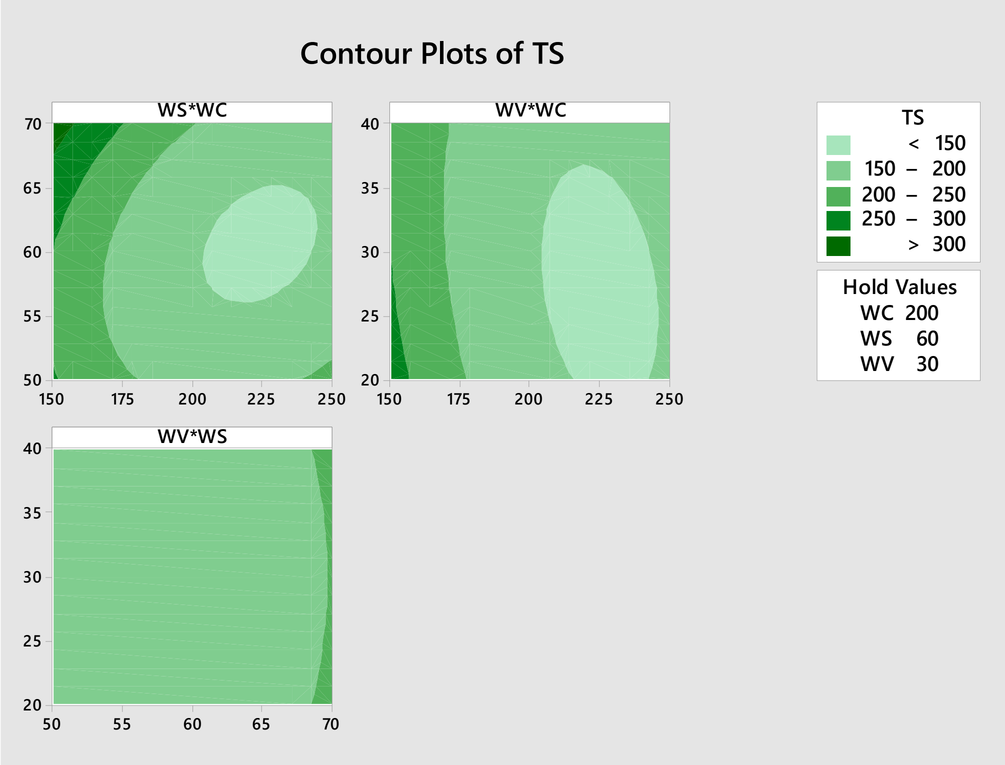

Fig. 4 Contour plot for TS

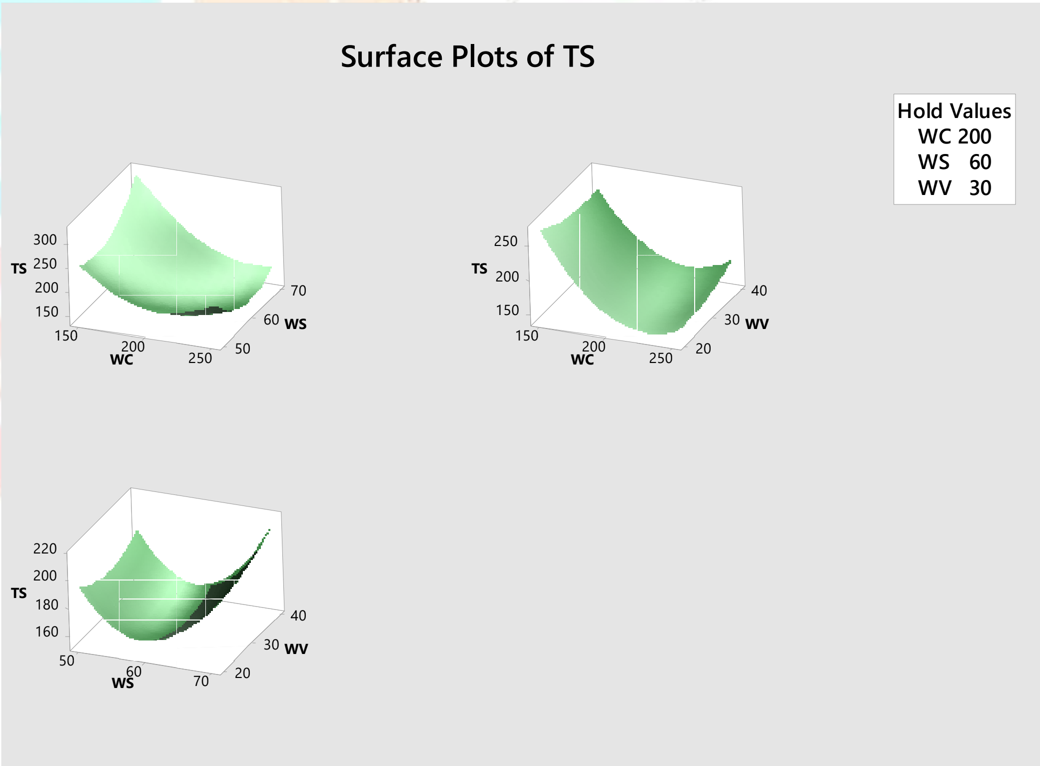

Fig. 5 Surface plot for TS

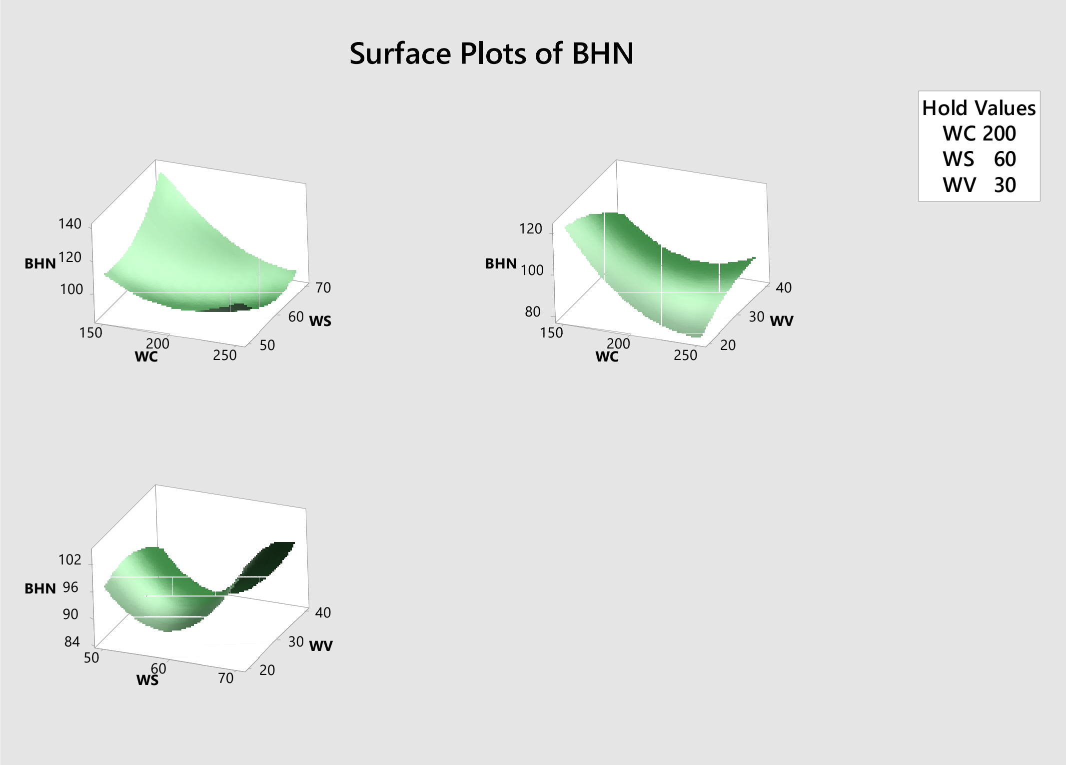

Fig. 6 Surface plot for BHN

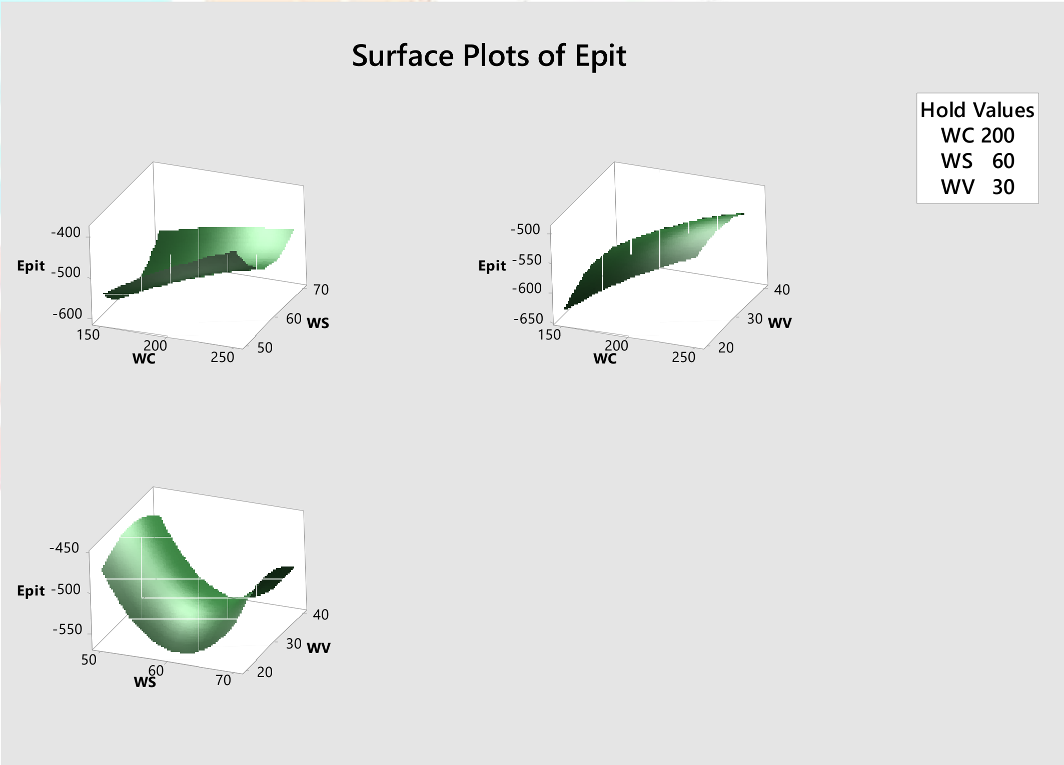

Fig. 7 Surface plot for CR

IV. RESULTS AND DISCUSSION

4.1 Microstructure of fusion zone

During the fabrication of welds using the GTA welding technique, large columnar grains were observed in the fusion zone. Because AA2219 alloy has a larger freezing range than most other alloys, the fusion zone is more prone to the formation of columnar dendrites. However, in GTAW, the weld pool is not agitated sufficiently to break the dendritic tips, as a result, there is no grain refinement to be found. Optical micrographs investigations revealed that the eutectic network in the fusion zone of the GTA weld is continuous (Fig. 8). There was a significant amount of copper segregation along grain boundaries. This can be explained by the significant temperature difference in the weld pool of the GTAW, which produces columnar growth of dendrites in the process of welding.

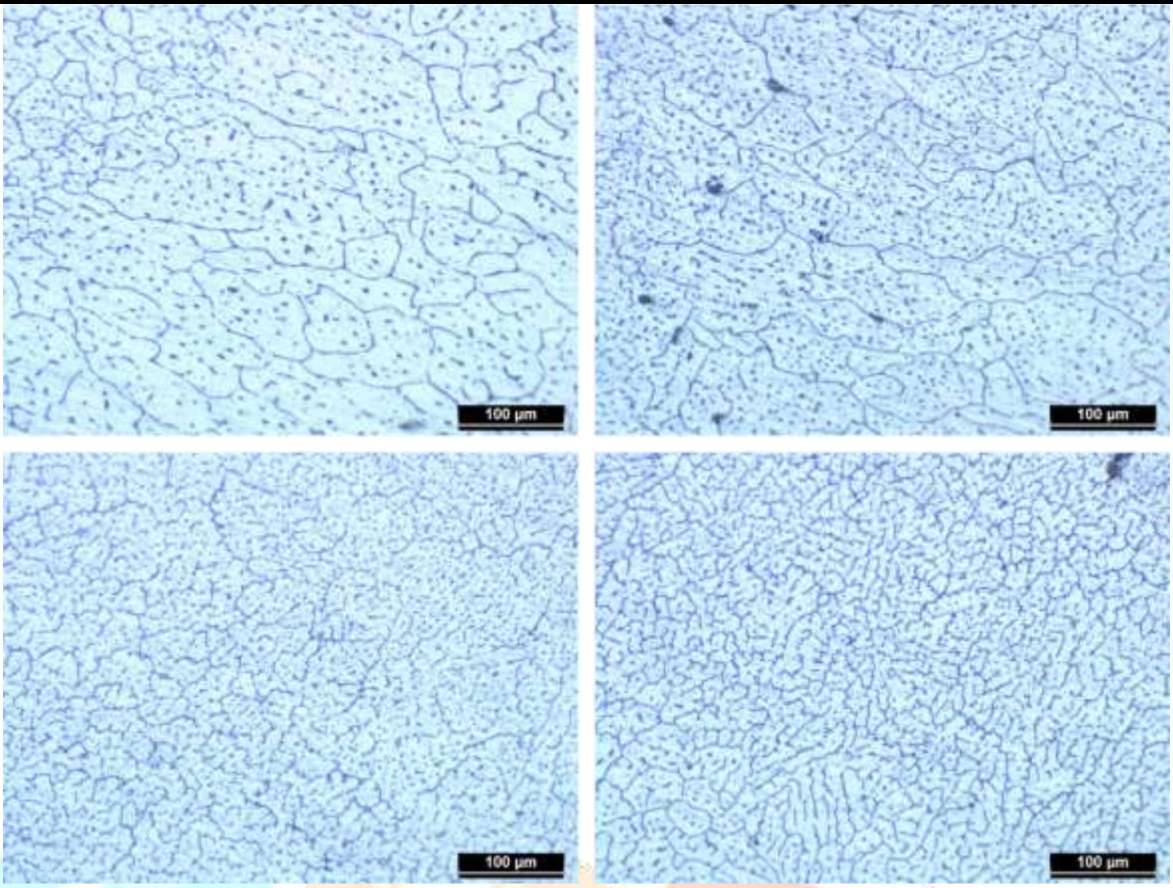

Fig. 8 Optical microstructures of GTAW AA2219 weld samples.

The weld zone's hardness is influenced by precipitate size and distribution. Indentation resistance is higher in copper rich precipitates at the grain boundaries. However, at grain boundaries in AA2219 Al-alloys are anodic to matrix and dissolution occurs [24]. Chain of precipitates at grain boundaries establishes galvanic coupling with the matrix and causes pitting corrosion. The corrosion behavior of the GTAW weld zone is expected to be different from corrosion in the base metal, and this may affect the long-term structural integrity of the GTA welded material. Specifically, the microstructural variations in the different GTAW zones are expected to produce galvanic effects that may induce localized corrosion, such as pitting. Galvanic interactions between intermetallics and the surrounding matrix produce local matrix disintegration, which results in pitting. When the passive layer on the material's surface damaged, it causes a massive discharge of electrons thereby sudden rise in current.

4.2. ANOVA analysis of variance

The most significant welding parameters that affect the corrosion resistance of GTAW AA2219 material were identified using analysis of variance (ANOVA). The ANOVA results are shown in Tables 4. The results of ANOVA indicate that WC is the process parameters that have significant contribution on the strength, hardness and corrosion resistance values of GTAW AA2219 material. In addition, a regression model by Minitab has been developed. The P-value of welding current is 0.034, 0.010 and 0.002 for TS, BHN and CR respectively which is most significant factor whereas the P-value for transitional speed and voltage is greater than 0.05 which indicates that these are less significant factor at 95% confidence level. In this case, WC (welding current) is most effective parameter which effects the responses of AA2219 aluminium alloy. The control variables are not significant if the P value is higher than 0.1. The "Predicted R-Squared" of for all the responses agrees with the "Adjusted R Squared" indicating a good fitness of the model.

Table 4 ANOVA results

Source	**DOF**	**Sum of squares**			**Mean square**			**F value**			**P value**		
		TS	**BHN**	**CR**	**TS**	**BHN**	**CR**	**TS**	**BHN**	**CR**	**TS**	**BHN**	**CR**
WC	2	18062	1286	17354	9030	643	8677	16.3	6.96	9.4	0.034	0.01	0.002
WS	2	4201	436	9016	2100	218	4508	3.8	2.36	4.9	0.21	0.3	0.173
WV	2	2125	69.5	898	1062	34.7	449	1.92	0.38	0.5	0.34	0.73	0.675

4.3 Response Optimization:

From table 5 the optimum combination values of strength, hardness and corrosion resistance 324.05 Mpa, 137.53 BHN and -527.741 mV respectively are obtain at welding current (WC) 150 A, transitional speed (WS) 70 mm/min and voltage (WV) is 31.68 V respectively. These optimum combinations of responses are obtained from the highest composite desirability of multi response optimization. Fig. 9 shows response optimizer plot also indicating the optimum welding parameters for combined effect of responses of GTA welded AA2219 aluminium alloy.

Table 5 Response Optimization

Solution	WC	WS	WV	Epit Fit	BHN Fit	TS Fit	Composite Desirability
1	150	70.0000	31.6857	-527.741	137.530	324.054	0.735027
2	150	70.0000	37.8247	-535.509	129.439	322.746	0.706688
3	250	50.0000	40.0000	-415.000	110.000	235.000	0.675858
4	250	50.0000	40.0000	-415.000	110.000	235.000	0.675858
5	250	50.5654	40.0000	-424.795	108.394	229.568	0.636686
6	250	50.0000	25.7759	-384.271	104.304	211.786	0.562029
7	250	50.0000	21.6957	-390.891	100.305	212.222	0.530692
8	250	50.0000	20.0000	-395.667	98.333	213.333	0.516224
9	250	70.0000	40.0000	-502.333	94.667	198.333	0.351889

Optimal Variable Setting

WC = 150 A
WS = 70 mm/min
WV = 31.68 V

Tensile strength = 324 Mpa
Hardness = 137.53 BHN
Corrosion Resistance = -527.741 mV

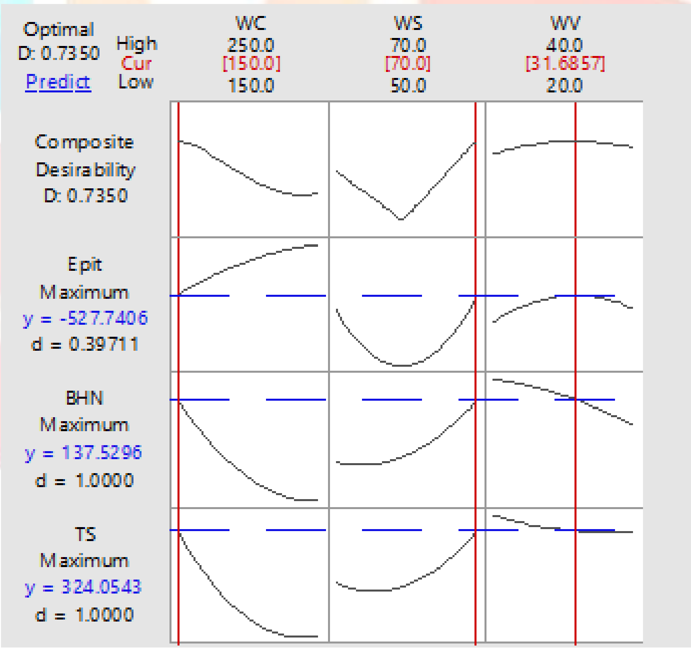

Fig. 9. Response Optimizer

V. CONCLUSIONS

1. From the ANOVA results the most significant parameter has welding current whereas transitional speed and voltage has least significant on the tensile strength, hardness and corossion resistance of AA2219 aluminium alloy
2. Microstructure study revealed that finer grains and continuous precipitates at grain boundaries trigger greater pitting corrosion of weld samples.
3. Using RSM, the developed regression model was able to predict the corrosion resistance of GTA welded AA2219 at 95% confidence level.
4. The RSM was utilized to maximize strength, hardness and corrosion resistance of the GTA welding parameters.
5. The optimum values of GTA welding parameters are welding current 150 A, transitional speed 70 mm/mim and voltage is 31.68 kV respectively.
6. The interaction effect of each parameter of the GTAW was studied by using response surface and contour graphs.

Acknowledgements

Authors express their gratitude to Department of metallurgical engineering, Andhra University, Visakhapatnam for their kind help in conducting welding experiments.

References:

1. Heinz, A., A. Haszler, C. Keidel, S. Moldenhauer, R. Benedictus, and W. S. Miller. "Recent development in aluminium alloys for aerospace applications." Materials Science and Engineering: A 280, no. 1 (2000): 102-107.
2. Dursun, Tolga, and Costas Soutis. "Recent developments in advanced aircraft aluminium alloys." Materials & Design (1980-2015) 56 (2014): 862-871.
3. Rambabu, P. P. N. K. V., N. Eswara Prasad, V. V. Kutumbarao, and R. J. H. Wanhill. "Aluminium alloys for aerospace applications." Aerospace materials and material technologies (2017): 29-52.
4. Verma, Rajesh P., and Manish Kumar Lila. "A short review on aluminium alloys and welding in structural applications." Materials Today: Proceedings 46 (2021): 10687-10691.
5. Grbović, Aleksandar, Zijah Burzić, and Srđa Perković. "Influence of Corrosion on Parameters of Fracture Mechanics of Aluminium Alloys 2024-T351 and 7075-T651." Tehnički vjesnik 29, no. 1 (2022): 239-245.
6. Kumar, Ravi, and N. K. Singh. "Modelling and Simulation on Behaviours of Aluminium Alloys." In Advances in Mechanical and Materials Technology, pp. 703-711. Springer, Singapore, 2022.
7. Banerjee, Sanjib, Rakesh Bhadra, and Sanjib Gogoi. "Investigating Weldability in Microalloyed Al Alloys." In Advances in Mechanical Engineering, pp. 271-279. Springer, Singapore, 2020.
8. Koona, Bhavani, VSN Venkata Ramana, Ch Prasad, and K. Sri Ram Vikas. "Comparison of microstructure and corrosion behaviour of AA2014 electron beam and friction stir welds." Materials Today: Proceedings (2021).
9. Jebaraj, A. Vinoth, K. V. V. Aditya, T. Sampath Kumar, L. Ajaykumar, and C. R. Deepak. "Mechanical and corrosion behaviour of aluminum alloy 5083 and its weldment for marine applications." Materials Today: Proceedings 22 (2020): 1470-1478.
10. Naik, D. Balaji, CH Venkata Rao, K. Srinivasa Rao, G. Madhusudan Reddy, and G. Rambabu. "Optimization of friction stir welding parameters to improve corrosion resistance and hardness of AA2219 aluminum alloy welds." Materials Today: Proceedings 15 (2019): 76-83.
11. Sriba, Amina, and Jean-Bernard Vogt. "Galvanic Coupling Effect on Pitting Corrosion of 316L Austenitic Stainless Steel Welded Joints." Metals and Materials International 27, no. 12 (2021): 5258-5267.
12. Srinivasa Rao, K., and K. Prasad Rao. "Corrosion resistance of AA2219 aluminium alloy: electrochemical polarisation and impedance study." Materials science and technology 22, no. 1 (2006): 97-104.
13. Brennecke, M. W. "Electron beam welded heavy gage aluminum alloy 2219." (1965).
14. Trzil, J. P., and D. W. Hood. "ELECTRON BEAM WELDING 2219-ALUMINUM ALLOY FOR PRESSURE VESSEL APPLICATIONS." Welding Journal 48, no. 9 (1969): S395.
15. Rao, SR Koteswara, G. Madhusudhan Reddy, K. Srinivasa Rao, M. Kamaraj, and K. Prasad Rao. "Reasons for superior mechanical and corrosion properties of 2219 aluminum alloy electron beam welds." Materials characterization 55, no. 4-5 (2005): 345-354.
16. Juang, S. C., and Y. S. Tarng. "Process parameter selection for optimizing the weld pool geometry in the tungsten inert gas welding of stainless steel." *Journal of materials processing technology* 122.1 (2002): 33-37.
17. Munoz, A. C., Rückert, G., Huneau, B., Sauvage, X., & Marya, S. (2008). Comparison of TIG welded and friction stir welded Al–4.5 Mg–0.26 Sc alloy. Journal of materials processing technology, 197(1-3), 337-343.
18. Peel M, Steuwer A, Preuss M, Withers PJ. Microstructure, mechanical properties and residual stresses as a function of welding speed in AA5083 friction stir welds. Acta Mater 2003;51:4791–801.
19. Sobih, Mohamed, Zuhair Elseddig, Khalid Almazy, and Mohamed Sallam. "Experimental Evaluation and Characterization of Electron Beam Welding of 2219 AL-Alloy." Indian Journal of Materials Science 2016 (2016).
20. Wang, Jian, Zhiyi Liu, Song Bai, Jing Cao, Juangang Zhao, Lei Luo, and Junlin Li. "Microstructure evolution and mechanical properties of the electron-beam welded joints of cast Al–Cu–Mg–Ag alloy." Materials Science and Engineering: A 801 (2021): 140363.
21. Xu, Weifeng, and Jinhe Liu. "Microstructure and pitting corrosion of friction stir welded joints in 2219-O aluminum alloy thick plate." Corrosion Science 51, no. 11 (2009): 2743-2751.
22. Rekab, Kamel, and Muzaffar Shaikh. Statistical design of experiments with engineering applications. Vol. 252. Boca Raton, FL: Taylor & Francis, 2005.
23. Montgomery, Douglas C. Design and analysis of experiments. John wiley & sons, 2017.
24. Trishul, M. A., and Bijayani Panda. "A Review on the Challenges in Welding of Aluminium AA2219 Alloy." In Advances in Lightweight Materials and Structures, pp. 663-671. Springer, Singapore, 2020.